Paper ID: TE-05

Natural convection in circular headed cavity with discrete bottom heat sources filled with Ferro-fluid

Anwarul Karim [1,*], Asif Reza Chowdhury [1], Khan Md. Rabbi [1]
[1] Department of Mechanical Engineering, Bangladesh University of Engineering and Technology
*E-mail: anwarul2buet@gmail.com *, rezaasif93@gmail.com , khanrabbi92@gmail.com*

Abstract

Natural convection in a two dimensional circular headed cavity filled with Ferro-fluid (water + Fe_3O_4) is numerically investigated for different heater positions. In this study, two discrete heat sources at constant temperature are located on the bottom wall. The vertical and circular top walls are cooled at constant low temperature. The Ferro-fluid is assumed to be homogenous and Newtonian. The physical problem is represented mathematically by sets of governing equations and the developed mathematical model is solved by employing Galerkin finite element formulation. The influence of pertinent parameter such as Rayleigh number (Ra) ranges from 10^3 to 10^6 for different aspect ratios (λ) of 0, 0.4 and 0.7 and also the solid volume fraction of Ferro-fluid (φ) from 0 to 0.15 on heat transfer are studied. The present study analyzes and discusses the flow patterns (streamline structures and isotherm distributions) set up by the buoyancy force and the heat transfer rate is quantified by the average Nusselt number (Nu) along the heat source. The results show that the heat transfer rate increases with the increase of the Rayleigh number and solid volume fraction of Ferro-fluid. It is also evident from results that heat transfer is maximum for $\lambda=0.7$ up to $Ra=10^6$ but the increasing rate of heat transfer is higher for $\lambda=0.4$ beyond $Ra=10^4$.

Keywords: Circular headed cavity, Natural convection, Ferro-fluid , Discrete heat source.

1. Introduction

Natural convection heat transfer is significantly applied in various fields like industries, scientific and engineering applications. Researchers have begun to experimentally and numerically investigate the natural convection of nanofluid in recent few years in order to extract the advantages of nanofluid. The numerical method to analyze natural convection in square cavity was first used by Vahl Davis [1]. Further natural convection for different cavities were investigated widely [2-4]. Choi [5] first found the term "Nanofluid". Nanofluid is suspension of nanoparticles (size up to about 1-100nm) in a base fluid as they exhibit enhanced thermal conductivity and convective heat transfer coefficient compared to the base fluid. The variety of nanofluid advantages can be related in many natural convection heat transfer applications such as in micro-electro-mechanical systems (MEMS), in heat exchangers,boilers,cooling engines,in fuel cells, solar energy,crystal growth etc. Ferrofluid is a stable colloidal suspension of sub-domain magnetic particles in a base liquid. The particles are coated with a stabilizing dispersing agent, which prevents particle agglomeration even when a strong magnetic field gradient is applied to the ferrofluid [6, 7]. The shape of cavity is also a considerable factor affecting the heat transfer and fluid flow phenomena. The variety of shape actually depends on the real life physical problems. The common shapes are square, rectangular, circular etc. The effect of multiple sources also has immense influence on heat transfer. Effect of multiple sources and sinks on natural convection is investigated with importance [8-10].

The literature reviews show that despite lots of work on convection, there is lack of information on effect of heater position along with ferro-fluid for cavity having circular head. In this paperwork, a ferrofluid filled circular headed cavity with discrete bottom heat sources is investigated for different positions of heat sources (aspect ratio). The effect of different Rayleigh number for different aspect ratios is shown in terms of flow and thermal field. Heat transfer effectiveness and average temperature are also presented in result. The model has been validated against established results and the results have been briefly discussed.

2. Problem formulation

2.1 Physical modeling

The geometry of the problem is depicted in *Fig.1*. The system consists of a two-dimensional cavity of sides *L* and the top circular head of diameter *L*. The bottom surface is heated by two heat sources of constant high temperature T_h. The vertical side walls and circular top wall are kept at constant low temperature T_c (< T_h) and the remaining walls are adiabatic. The length of each heat source is *a* and the difference between them is *b*. The ratio *b/L* is taken as aspect ratio which is varied as *0, 0.4* and *0.7*. The entire cavity is filled with ferrofluid *(water + Fe_3O_4)*. The gravity is acting in the negative y-direction. The radiation effect and viscous dissipation are neglected for the simplification of the problem.

Nomenclature

g	acceleration due to gravity (m/s^{-2})	Greek symbol	
k	thermal conductivity ($W\ m^{-1}K^{-1}$)	λ	aspect ratio (b/L)
T	temperature (K)	ρ	density (kgm^{-3})
L	length of the cavity (m)	α	thermal diffusivity (m^2s^{-1})
p	pressure (Pa)	β	volume expansion coefficient (K^{-1})
P	dimensionless pressure	ν	kinematic viscosity (m^2s^{-1})
(u, v)	velocity components (ms^{-1})	φ	solid volume fraction
(U, V)	dimensionless velocity components	Ψ	stream function
(x, y)	dimensional coordinates (m)	Θ	dimensionless temperature
(X, Y)	dimensionless coordinates	Subscript	
Ra	Rayleigh number	h	hot
Pr	Prandtl number	c	cold
Nu	Nusselt number	ff	ferrofluid

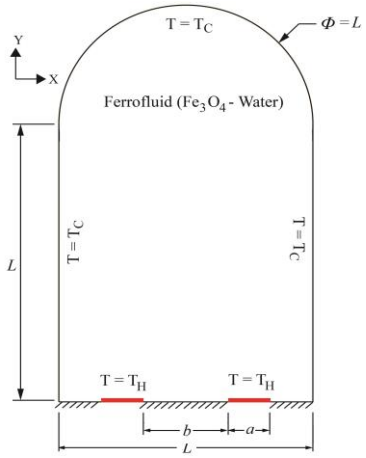

Fig. 1. Schematic diagram of circular headed cavity with discrete heat source.

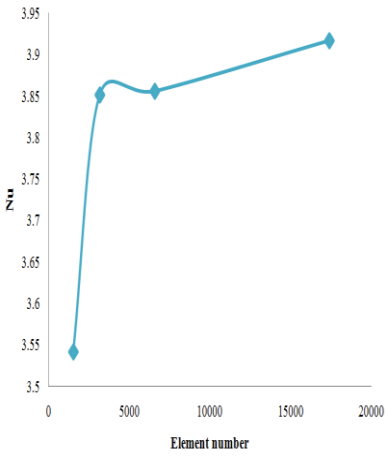

Fig. 2. Grid refinement test on average Nusselt number for $Ra=10^5$ and φ=0.1.

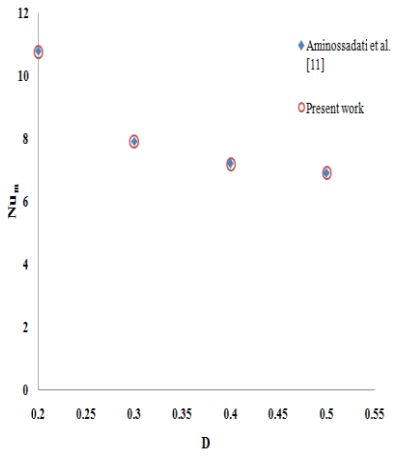

Fig. 3. Comparison of present work with Aminossadati et al. [11] for $Ra=10^5$, φ=0.1 and B=0.4.

2.2 Mathematical modeling

The two-dimensional steady state continuity, momentum and energy equations are applied to model this problem for flow and thermal fields. The working fluid is assumed to be incompressible Newtonian with constant properties and thermal equilibrium between the ferromagnetic particles and the base fluid are assumed. The density variation of the fluid is modeled by the Boussinesq approximation by the buoyancy term.

From the above stated assumptions, the non-dimensional governing equations take the form as-

$$\frac{\partial(U\delta)}{\partial X}+\frac{\partial(V\delta)}{\partial Y}=\frac{\partial}{\partial X}\left(\Gamma_\delta\frac{\partial\delta}{\partial X}\right)+\frac{\partial}{\partial Y}\left(\Gamma_\delta\frac{\partial\delta}{\partial Y}\right)+S_\delta \qquad (1)$$

Here non-dimensional dependent variables are designated by δ and corresponding diffusion and source term are defined by Γ_δ and S_δ respectively and those are summarized in Table 1,

Table 1. A summary of the terms of the non-dimensional governing equations (1).

Equations	δ	Γ_δ	S_δ
Continuity	1	0	0
U-momentum	U	$\mu_{ff} / \rho_{ff} \alpha_f$	$-\partial P / \partial X$
V-momentum	V	$\mu_{ff} / \rho_{ff} \alpha_f$	$-\partial P / \partial Y + (\rho\beta)_{ff} Ra \Pr \Theta / (\rho_{ff} \beta_f)$
Thermal energy	Θ	α_{ff} / α_f	0

The non-dimensional parameters, which are adopted to obtain the above non-dimensional governing equation, are presented below-

$$X = \frac{x}{L}, Y = \frac{y}{L}, U = \frac{uL}{\alpha_f}, V = \frac{vL}{\alpha_f}, P = \frac{(p + \rho_f gy)L^2}{\rho_{ff} \alpha_f^{\ 2}}, \Theta = \frac{(T - T_c)}{(T_h - T_c)} \tag{2}$$

here U, V, P and Θ are non-dimensional velocities, pressure and temperature respectively. Here subscripts 'ff' and 'f' stand for the properties of the ferrofluid and the base fluid respectively.
The non-dimensional governing parameters Rayleigh number (Ra), Prandtl number (Pr) and Hartmann number (Ha) can be defined as below-

$$Ra = \frac{g\beta_f L^3 (T_h - T_c)}{\alpha_f \nu_f}, \Pr = \frac{\nu_f}{\alpha_f} \tag{3}$$

The density of ferrofluid which is assumed to be constant can be expressed as-

$$\rho_{ff} = (1-\varphi)\rho_f + \varphi\rho_s \tag{4}$$

Here property of solid ferromagnetic particles is represented by subscript's'. In the above equation, solid volume fraction (φ) has significant effect on thermal diffusivity of ferrofluid which is quite different from the base fluid and can be modeled as-

$$\alpha_{ff} = \frac{k_{ff}}{(\rho c_p)_{ff}} \tag{5}$$

where heat capacitance of ferrofluid $(\boldsymbol{\rho} c_p)_{ff}$ can be found by

$$(\rho c_p)_{ff} = (1-\varphi)(\rho c_p)_{ff} + \varphi(\rho c_p)_s \tag{6}$$

In addition, the thermal expansion coefficient (β_{ff}) of the ferrofluid can be obtained as

$$(\rho\beta)_{ff} = (1-\varphi)(\rho\beta)_{ff} + \varphi(\rho\beta)_s \tag{7}$$

Moreover, dynamic viscosity of the ferrofluid (μ_{ff}) can be expressed as

$$\mu_{ff} = \frac{\mu_f}{(1-\varphi)^{2.5}} \tag{8}$$

Effect of thermal conductivity of ferrofluid can be described as

$$\frac{k_{ff}}{k_f} = \frac{k_s + 2k_f - 2\varphi(k_f - k_s)}{k_s + 2k_f + \varphi(k_f - k_s)} \tag{9}$$

The thermophysical properties of the base fluid (kerosene) and the ferromagnetic particle (cobalt) are given in Table 2.

Table 2. Thermophysical properties of ferrofluid.

Property	Fe_3O_4 (nanoparticles)	Water (base fluid)
Heat capacitance, c_p ($JKg^{-1}K^{-1}$)	670	4179
Density, ρ (Kgm^{-3})	5200	997.1
Thermal conductivity, k ($Wm^{-1}K^{-1}$)	6	0.613
Thermal expansion coefficient, β (K^{-1})	1.18×10^{-5}	2.1×10^{-4}
Dynamic viscosity, μ (Nsm^{-2})	-	0.001003

The corresponding dimensionless boundary conditions for the above problem are given by:
On vertical walls: U=0, V=0, Θ=0.

On top circular wall: U=0, V=0, Θ=0.
On bottom wall: U=0, V=0, Θ=1 (at heat sources) or $\partial\Theta / \partial Y = 0$ *(at wall other than sources).*
Average Nusselt number is evaluated for horizontal bottom heated walls and calculated from following expression

$$\mathrm{Nu} = -\frac{\mathrm{k_{ff}}}{\mathrm{k_f}} \int_0^1 \frac{\partial \Theta}{\partial \mathrm{y}} \mathrm{d\,X} \tag{10}$$

Average fluid temperature inside the cavity can also be found by the following expression

$$\Theta_{\mathrm{av}} = \frac{1}{\mathrm{A}} \int \Theta \mathrm{dA} \tag{11}$$

where A is non dimensional area which can be evaluated by $A=L^2(1+\pi/8)$.
Flow field of the present problem is visualized through streamline obtained from stream function. Stream function is defined from velocity components U and V. Relation between the stream function and velocity components for 2-D flow are given by,

$$\mathrm{U} = \frac{\partial \psi}{\partial \mathrm{Y}}, \mathrm{V} = -\frac{\partial \psi}{\partial \mathrm{X}} \tag{12}$$

3. Numerical procedure

Galerkin weighted residual method of finite element analysis is applied study to obtain the numerical solution. The entire domain is discritized into triangular mesh elements of different size. Non-dimensional governing equations are transformed into a set of algebraic equations. $P_2 - P_1$ Lagrange finite elements are used to discretize pressure and velocity components and Lagrange-quadratic finite elements are chosen for temperature. Iteration technique is employed to find the converged solution. The convergence criterion is set to 10^{-6}, so that $| z^{p+1} - z^{p} | \leq 10^{-6}$, where *z* is the general dependent variable and *p* is the number of iteration.

4. Grid independency test

A grid sensitivity test is performed for $Ra=10^5$ and $\varphi=0.1$ for aspect ratio of λ=0.4 to ensure the numerical accuracy of this computation. The test is performed for different element numbers as 1528, 3167, 6576 and 17393. It is evident from *Fig.2* that after reaching element number 6576, average Nusselt number becomes insensitive. So for the present problem, grid having element number 6576 is taken as the optimum grid and all the simulations are carried out at this specified grid.

5. Code validation

A code validation is necessary for checking the reliability of the present code. The present code is compared with the results of Aminossadati et al. [11] on the basis of average Nusselt number for $Ra=10^5$ and φ=0.1 where heat source length B=0.4. As indicated from *Fig.3*, obtained result shows good agreement with literature result.

6. Result and discussion

The main objective of investigation is to analyze the effect of different heater configurations on natural convection for varying Rayleigh number inside a circular headed cavity filled with ferro fluid. Heat transfer performance is compared for aspect ratios (λ) of 0, 0.4 and 0.7 while varying Raleigh number from 10^3 to 10^6 with constant solid volume fraction φ=0.02 in terms of streamline and isotherm contours, average Nusselt number (*Nu*) and average temperature (θ_{av}) of the fluid inside cavity. The effect of different solid volume fraction (φ=0, 0.05, 0.07, 0.1 and 0.15) is also quantified for various Rayleigh number.

6.1 Effect of Rayleigh number on different aspect ratio

Effect of Rayleigh number (*Ra*) on flow and thermal fields for aspect ratio *λ=0, 0.4 and 0.7* is depicted in terms of stream function and isothermal contours in *Fig.4*. The study is carried out for solid volume fraction of *φ=0.02* and *Ra= 10^3, $10^5$and 10^6*. A counter clockwise (CCW) vortex at left and a clockwise (CW) vortex at right half of cavity are evaluated for all *λ* for $Ra=10^3$. But the vortices for *λ=0.7* is more elongated in vertical direction compared to other two aspect ratios. This leads to higher buoyancy effect when the distance between the sources are maximum (*λ=0.7).* The isotherm contours are stratified in parallel lines for *λ=0* which are a bit distorted for *λ=0.4* and *0.7*. The vortices are stretched vertically for all *λ* when $Ra=10^5$ in *Fig.4 [(g)~(i)]*. For the distant heater position, streamline elongated most. The isotherm contours also show immense changes as Ra updated to 10^5. The isotherms near heater become thinner which indicates increasing convection heat transfer. The greater deflection of isotherms is noticed in case of *λ=0.4*. This indicates rapid growth of heat transfer rate for *λ=0.4* when $Ra=10^5$. The vortices engulf almost all the cavity as Rayleigh number is updated to 10^6 for all λ at *Fig.4 [*

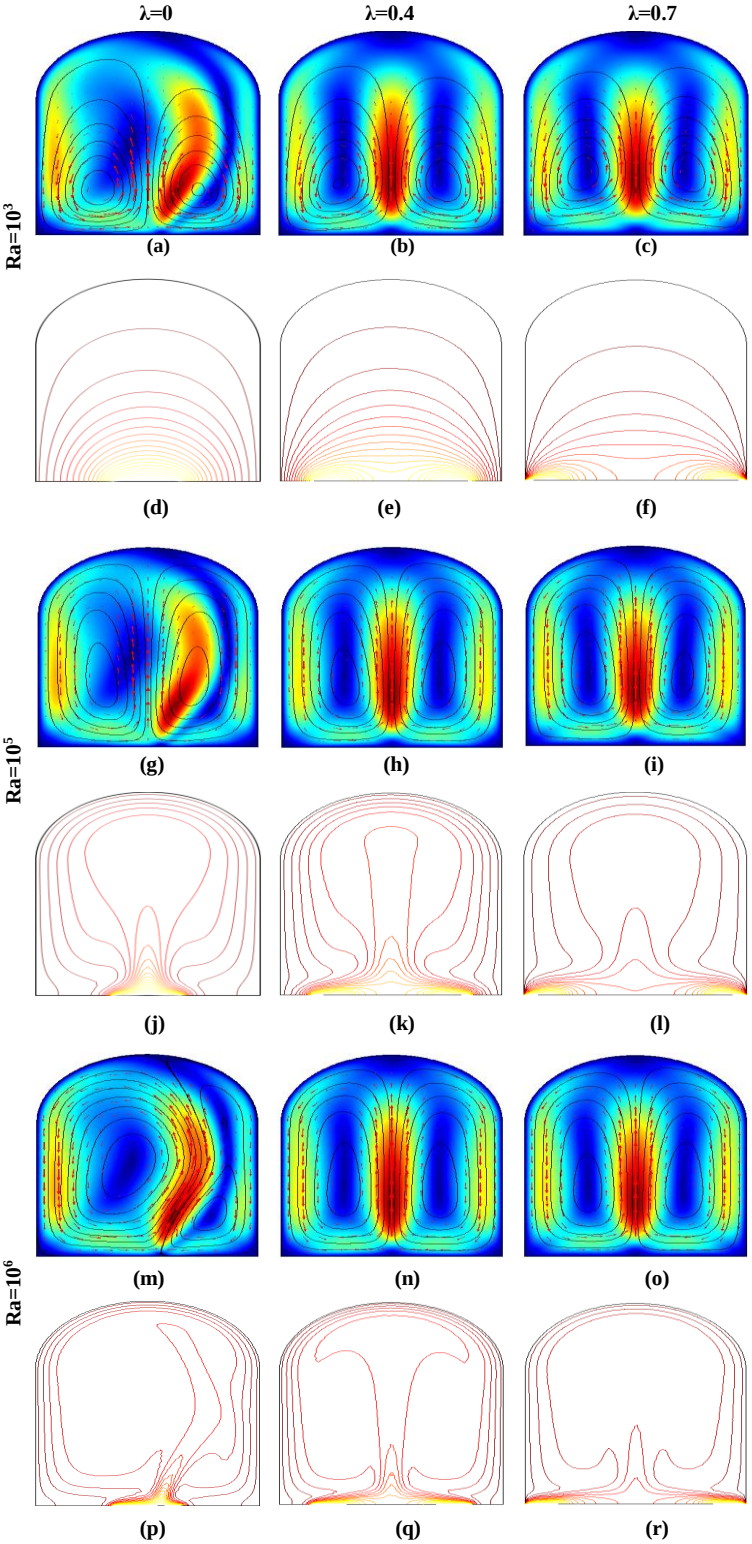

Fig.4 Variation of streamlines for Ra=10^3 at [(a), (b), (c)]; Ra=10^5 at [(g), (h), (i)]; Ra=10^6 at [(m), (n), (o)] and isotherm contours for Ra=10^3 at [(d), (e), (f)]; Ra=10^5 at [(j), (k), (l)]; Ra=10^6 at [(p), (q), (r)]

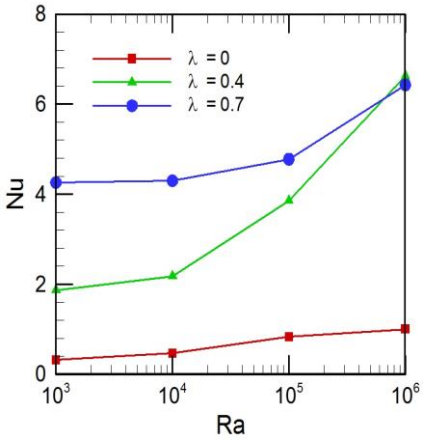

Fig.5 Variation of *Nu* with *Ra* for λ=0, 0.4 and 0.7

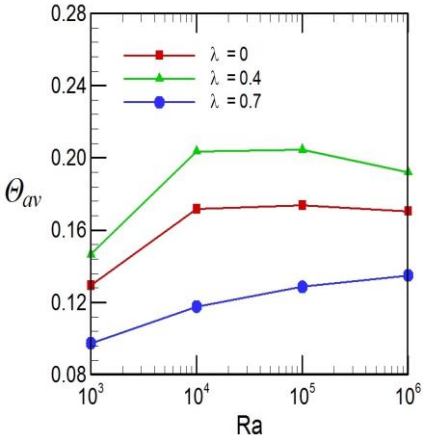

Fig.6 Variation of Θ_{av} with *Ra* for λ=0, 0.4 and 0.7

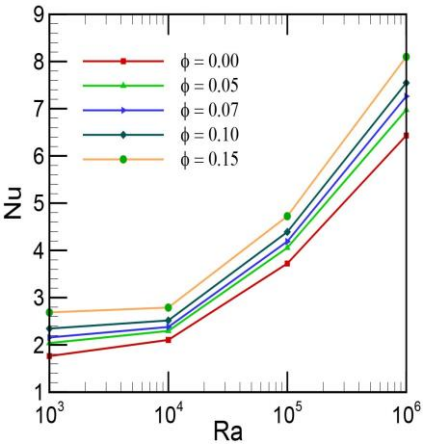

Fig.7 Variation of *Nu* with *Ra* for φ=0, 0.05, 0.07, 0.1 and 0.15

(m) ~(r)]. For *λ=0* the left side vortex elongated more in vertically and horizontally indicating that convection is dominant in CCW direction in this case. The streamline patterns are almost same for the other two aspect ratios. The isotherm lines become thinner than previous which represents higher convection in all λ. The distortion of isotherms is noticeable for *λ=0*. For *λ=0.4* isotherms diffuse through the entire cavity which denotes the increasing rate of convection. Heat transfer also increases in case of *λ=0.7* as the thermal boundary layer becomes thinner.

6.2 Variation of Nusselt number and average temperature

Nusselt number defines the effectiveness of convection heat transfer. The variation of Nusselt number with Rayleigh number for various aspect ratio ($\lambda=0, 0.4, 0.7$) is depicted in *Fig.5*. It is seen from the figure that Nu value increases as Ra increase. Nu value is maximum for $\lambda=0.7$ up to $Ra<10^6$. This implies that heat transfer is maximum when the heat sources are in distant position. The minimum heat transfer happens for $\lambda=0$ when the sources are in close position. It is also noticed that the increasing rate of convection is higher for $\lambda=0.4$. The average temperature inside the cavity increases for increment of $Ra=10^3$ to $Ra=10^4$ and more or less constant for further increasing value of Ra for all three aspect ratios seen from *Fig.6*. Maximum average temperature is found for $\lambda=0.4$ and the minimum for $\lambda=0.7$.

6.3 Effect of solid volume fraction

The effect of solid volume fraction of ferrofluid (φ) on heat transfer is shown in *Fig.7*. For φ of 0, 0.05, 0.07, 0.1 and 0.15 Nusselt number is found for different *Ra*. The graph indicates that higher solid volume fraction results in higher *Nu* i.e. higher convection heat transfer. This indicates that the addition of more nanoparticle (Fe_3O_4) with base fluid increases fluid solid interaction hence increases convection.

7. Conclusion

The results of numerical analysis on flow field, thermal field and effectiveness of heat transfer with varying Rayleigh number for different aspect ratio and solid volume fraction are computationally analyzed in a ferrofluid filled circular headed cavity with discrete heat sources. The outcomes are listed as follows:

- Heat transfer increases with Rayleigh number for all heater positions or aspect ratio.
- The configuration of heat sources in distant position ($\lambda=0.7$) provides better heat transfer than the adjacent one ($\lambda=0$). But heat transfer rate is rapid for $\lambda=0.4$.
- The addition of ferro particle (increasing solid volume fraction) increases heat transfer significantly.

8. References

[1] de Vahl Davis, G. "Natural convection of air in a square cavity: a bench mark numerical solution." International Journal for numerical methods in fluids 3.3 (1983): 249-264.

[2] Dixit, H. N., and V. Babu. "Simulation of high Rayleigh number natural convection in a square cavity using the lattice Boltzmann method." International journal of heat and mass transfer 49.3 (2006): 727-739.

[3] Oztop, Hakan F., and Eiyad Abu-Nada. "Numerical study of natural convection in partially heated rectangular enclosures filled with nanofluids." International Journal of Heat and Fluid Flow 29.5 (2008): 1326-1336.

[4] Grosan, T., et al. "Magnetic field and internal heat generation effects on the free convection in a rectangular cavity filled with a porous medium." International Journal of Heat and Mass Transfer 52.5 (2009): 1525-1533.

[5] S.U.S. Choi, J.A. Eastman, Enhancing thermal conductivity of fluids with nanoparticles, in: Proceedings of the 1995 ASME Int. Mech. Eng. Cong. And Expo, ASME, San Francisco, USA, (1995).

[6] C. Chang, W.Cheng, W.Liu, H.Cheng, C.Huang, S.Du, Thermal flow of fluid with magnetic particles in the presence of magnetic field, Int.Commun.Heat Mass Transfer37(2010)801–808.

[7] M. Ghasemian,Z.Najafian Ashrafi, M.Goharkhah,M.Ashjaee, Heat transfer characteristics of Fe3O4 ferrofluid flowing in a mini channel under constant and alternating magnetic fields, Journal of Magnetism and Magnetic Materials 381(2015)158–167.

[8] V.C. Mariani, A. Da Silva, Natural convection: analysis of partially open enclosures with an internal heated source, Numer. Heat Transfer, Part A 52 (2007) 595–619.

[9] I. Dagtekin, H.F. Oztop, Natural convection heat transfer by heated partitions within enclosure, Int. Commun. Heat Mass Transfer 28 (2001) 823–834.

[10] Aminossadati, S. M., and B. Ghasemi. "Natural convection of water–CuO nanofluid in a cavity with two pairs of heat source–sink." *International Communications in Heat and Mass Transfer* 38.5 (2011): 672-678.

[11] Aminossadati, S. M., and B. Ghasemi. "Natural convection cooling of a localised heat source at the bottom of a nanofluid-filled enclosure." *European Journal of Mechanics-B/Fluids* 28.5 (2009): 630-640.